ЖЭТФ, 2015, том 147, вып. 2, стр. 240–247

DYNAMICS OF EXCITED INSTANTONS IN THE SYSTEM OF FORCED GURSEY NONLINEAR DIFFERENTIAL EQUATIONS

F. Aydogmus*

Department of Physics, Faculty of Science, Istanbul University
34452, Istanbul, Turkey

Received July 13, 2014

The Gursey model is a $4D$ conformally invariant pure fermionic model with a nonlinear spinor self-coupled term. Gursey proposed his model as a possible basis for a unitary description of elementary particles following the "Heisenberg dream". In this paper, we consider the system of Gursey nonlinear differential equations (GNDEs) formed by using the Heisenberg ansatz. We use it to understand how the behavior of spinor-type Gursey instantons can be affected by excitations. For this, the regular and chaotic numerical solutions of forced GNDEs are investigated by constructing their Poincaré sections in phase space. A hierarchical cluster analysis method for investigating the forced GNDEs is also presented.

DOI: 10.7868/S0044451015020054

1. INTRODUCTION

Solitons were discovered in the 19th century as nondissipating surface waves on water and were later realized to obey nonlinear wave equations [1]. During the past forty years, a rather complete description of solitons has been developed by the productive collaboration of mathematicians and physicists. In mathematical physics, the amount of information on nonlinear wave phenomena obtained using solitons is quite high. Today it is known that solitons play an important role in many areas, ranging from condensed matter physics to cosmology.

There are four leading soliton types: instanton, monopole, vortex, and kink ones. Instantons have a finite action with zero energy, and they have been considered as configurations of quantum fields that provide a tunnelling effect between the vacuums that have different topologies in space–time. This property of instantons is especially interpreted to overcome the quark confinement problem. Before the instanton solutions were discovered in 1975 by Belavin, Polyakov, Schwarz, and Tyupkin [2] in the Yang–Mills theory, this theory of strong interactions appeared to have a symmetry that did not exist in nature; this was known as the axial U(1) problem and was solved by 't Hooft, who realized that it may even be the most important effect of instanton solutions to break the unwanted symmetry [3]. This was the first example of an extended classical solution having a physical consequence in the field theory of particle physics. In recent years, one of the most powerful uses of instantons is in the various topics of both QCD and electroweak theory. Although they play an important role in the interface region between partonic and hadronic description of strong interactions theoretically, direct experimental evidences for instantons have being lacking until now. However, a careful analysis of Large Hadron Collider (LHC) data at CERN might bring experimental confirmation of such processes [4].

After the success of the Dirac equation in the description of electron dynamics, the first work on models including only spinors goes back to Heisenberg [5]. Heisenberg spent his years to formulate a "theory of everything" using only fermions. A few decades later, as a possible basis for a unitary description of elementary particles, Gursey proposed a new spinor wave equation that is similar to Heisenberg's nonlinear generalization of the Dirac equation but in addition exhibits invariance with respect to conformal transformations [6]. Gursey had to use a nonpolynomial form in order to write a conformally invariant Lagrangian. Gursey's model possesses broader dynamical symmetries compared to Dirac's and Heisenberg et al.'s works. More importantly, Gursey's work is suitable for extensions to other particles with spin [6]. In the same year, Ko-

*E-mail: fatma.aydogmus@gmail.com

rtel found some classical solutions of Gursey's conformal invariant spinor wave equation via the Heisenberg ansatz [5, 7], which much later were shown to be instantons (Gursey instantons) by considering conformal symmetry breaking, which means that $\langle 0|\overline{\psi}\psi|0\rangle \neq 0$ [8]. The Gursey model is very important because of the similarity of these solutions to solutions of pure Yang–Mills theories in four dimensions. As a possible passage to the quantum level, the Poisson bracket structure of this model has also been proposed by the introduction of auxiliary scalar fields and using the Dirac method for constrained systems [9]. In Ref. [10], a Soler-type soliton solution [11] of the Gursey model with a mass term was given and its phase space behavior was investigated [12].

On the other hand, very recently, the stability behavior of Gursey instantons around their bifurcation points in phase space has been investigated by using the system of Gursey nonlinear differential equations (GNDEs) in a Euclidean configuration with the Heisenberg ansatz. Moreover, the role of the coupling constant has been discussed [13, 14].

In this paper, we again consider the GNDEs using the Heisenberg ansatz. We use this system to understand how the behavior of Gursey instantons can be affected by excitation. For this, we first look for the stability characterization of Gursey instantons and then investigate the regular and chaotic numerical solutions of forced GNDEs by constructing their Poincaré sections in phase space. We also built the bifurcation diagram of forced GNDEs to find the critical value of the forcing frequency as the control parameter. Besides this, a hierarchical cluster analysis method of investigation is presented to reinforce our conclusions.

2. GURSEY'S CONFORMAL INVARIANT SPINOR WAVE EQUATION AND INSTANTONS

The Gursey wave equation [6] is described by the conformal invariant Lagrangian

$$L = i\overline{\psi}\partial\!\!\!/\psi + g(\overline{\psi}\psi)^{4/3}, \tag{1}$$

where the fermion field ψ has scale dimension $3/2$ and g is a positive dimensionless coupling constant. The conformal invariant spinor wave equation that follows from the above Lagrangian is

$$i\gamma_\mu\partial_\mu\psi + g(\overline{\psi}\psi)^{1/3}\psi = 0. \tag{2}$$

In Ref. [15], $\overline{\psi}\psi$ for spinor-type instanton solutions are also related to spontaneous symmetry breaking of the full conformal group and $\overline{\psi}\psi$ is then characterized by being invariant under the transformations of a special subgroup [16], which in turn reflects the final symmetry properties of the ground state of the system as

$$R_\mu(\overline{\psi}\psi) \equiv \frac{i}{a}\left[\frac{a^2-x^2}{2}\,\partial_\mu + (x\partial + 2d)x_\mu\right](\overline{\psi}\psi) = 0, \tag{3}$$

where

$$R_\mu = \frac{1}{2}\left(aP_\mu + \frac{1}{a}D_\mu\right), \tag{4}$$

and a is a parameter with the dimensions of length, P_μ is the momentum operator, and D_μ is a conformal scale-invariant operator in the four-dimensional Euclidean space–time. We then find that

$$\overline{\psi}\psi = \pm\frac{a}{g(a^2+x^2)}$$

for a solution related to the special case (instanton) [15] of a Euclidean configuration of the Heisenberg ansatz [5]

$$\psi = \left[ix_\mu\gamma_\mu\chi(s) + \varphi(s)\right]c, \tag{5}$$

where c is an arbitrary spinor constant and $\chi(s)$ and $\varphi(s)$ are real functions of $s = x_\mu^2 = r^2 + t^2$ ($x_1 = x$, $x_2 = y$, $x_3 = z$, $x_4 = t$) in the Euclidean space–time, i. e., $r^2 = x_1^2 + x_2^2 + x_3^2$. Substituting Eq. (5) in Eq. (2) with

$$\begin{aligned} i\partial\!\!\!/\psi &= i\gamma_\mu\partial_\mu\psi = \\ &= \left[-4\chi(s) - 2s\frac{d\chi(s)}{ds} + 2ix_\mu\gamma_\mu\frac{d\varphi(s)}{ds}\right]\overline{c}c, \end{aligned} \tag{6}$$

and

$$(\overline{\psi}\psi)^{1/3} = \left(s\chi(s)^2 + \varphi(s)^2\right)(\overline{c}c)^{1/3}, \tag{7}$$

we obtain the system of nonlinear differential equations

$$\begin{aligned} &4\chi(s) + 2s\frac{d\chi(s)}{ds} - g(\overline{c}c)^{1/3} \times \\ &\qquad \times \left[s\chi(s)^2 + \varphi(s)^2\right]^{1/3}\varphi(s) = 0, \end{aligned} \tag{8a}$$

$$2\frac{d\varphi(s)}{ds} + g(\overline{c}c)^{1/3}\left[s\chi(s)^2 + \varphi(s)^2\right]^{1/3}\chi(s) = 0, \tag{8b}$$

where we write $\alpha = g(\overline{C}C)^{1/3}$ for brevity. Substituting $\chi = As^{-\sigma}F(u)$ and $\varphi = Bs^{-\tau}G(u)$, with $u = \ln s$ and $\sigma = \tau + 1/2$, $\tau = 3/4$, and $A^2 = B^2$ [7], we obtain the dimensionless form of the system of nonlinear ordinary coupled differential equations (8) as

$$\begin{aligned} &2\frac{dF(u)}{du} + \frac{3}{2}F(u) - \alpha(AB)^{1/3} \times \\ &\qquad \times \left[F(u)^2 + G(u)^2\right]^{1/3}G(u) = 0, \end{aligned} \tag{9a}$$

$$2\frac{dG(u)}{du} - \frac{3}{2}G(u) + \alpha(AB)^{1/3} \times \\ \times \left[F(u)^2 + G(u)^2\right]^{1/3} F(u) = 0, \quad (9b)$$

where F and G are dimensionless functions of u, and A and B are constants [7]. We call these equations the Gursey nonlinear differential equations (GNDEs) and the solutions of GNDEs with $\alpha(AB)^{1/3} = 1$ are the "Gursey instantons" given in [8]. It is difficult to obtain these exact solutions directly, and therefore numerical simulations were performed [13]. Moreover, the role of the coupling constant in the evolution of $4D$ spinor-type Gursey instantons in phase space has been investigated elsewhere via the Heisenberg ansatz [13, 14].

For the stability characterization of Gursey instantons, we find the fixed points of GNDEs as functions of $\alpha(AB)^{1/3}$. They are

$$\left(\pm\frac{3\sqrt{3/2}}{8[\alpha(AB)/3]^{3/2}}, \pm\frac{3\sqrt{3/2}}{8[\alpha(AB)/3]^{3/2}}\right). \quad (10)$$

The eigenvalues belonging to these fixed points are

$$\lambda_{\pm} = \pm\frac{1}{4}\left\{9 - \frac{16\alpha(AB)^{1/3}FG}{(F^2+G^2)^{2/3}} - \right. \\ \left. - \frac{80}{3}\alpha^2(AB)^{2/3}(F^2+G^2)^{2/3}\right\}^{1/2}. \quad (11)$$

Substituting the above fix points gives purely imaginary eigenvalues for all $\alpha(AB)^{1/3} > 0$. Hence, the equilibrium points are elliptic in character. An elliptic fixed point has a closed orbit around it [13, 14]. As can be seen from Fig. 1 (plotted for $\alpha(AB)^{1/3} = 1$), the phase-space dynamics of Gursey instantons has an undamped Duffing-type stability characteristic. This behavior does not depend on the values of the coupling constant [13, 14].

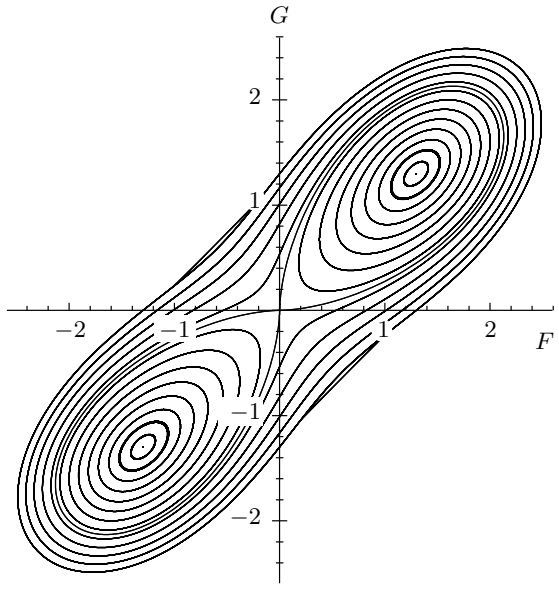

Fig. 1. Undamped Duffing-type stability characterization of Gursey instantons for $\alpha(AB)^{1/3} = 1$; the equilibrium points are $\left(-\frac{3\sqrt{3}}{4}, -\frac{3\sqrt{3}}{4}\right)$ and $\left(\frac{3\sqrt{3}}{4}, \frac{3\sqrt{3}}{4}\right)$

3. REGULAR AND CHAOTIC SOLUTIONS OF FORCED GNDEs

The main aim of this paper is to investigate the characteristics of forced GNDEs by reporting the Poincaré sections on the dimensionless phase space $(F(u), G(u))$ and the bifurcation diagram to see how the stable behavior of Gursey instantons can be affected by external forcing.

We redefine forced GNDEs by using a new constant $\beta \equiv \alpha(AB)^{1/3}$ as

$$2\frac{dF(u)}{du} + \frac{3}{2}F(u) - \\ - \beta\left[F(u)^2 + G(u)^2\right]^{1/3} G(u) = 0, \quad (12a)$$

$$2\frac{dG(u)}{du} - \frac{3}{2}G(u) + \\ + \beta\left[F(u)^2 + G(u)^2\right]^{1/3} F(u) = a\cos(\omega u). \quad (12b)$$

In the forced system, we can consider two main parameters: the amplitude and the frequency of excitation. Here, a is the amplitude of the external forcing and ω is its frequency. Forced GNDEs can be converted to

$$2\frac{dF(u)}{du} + \frac{3}{2}F(u) - \\ - \beta\left[F(u)^2 + G(u)^2\right]^{1/3} G(u) = 0, \quad (13a)$$

$$2\frac{dG(u)}{du} - \frac{3}{2}G(u) + \\ + \beta\left[F(u)^2 + G(u)^2\right]^{1/3} F(u) = a\cos[\omega H(u)], \quad (13b)$$

$$\frac{dH(u)}{du} = \Omega, \quad (13c)$$

with a constant Ω by adding an extra dimension for numerical calculations. When these forced GNDEs are considered as a flow, the vector field is

$$\mathbf{f} = \left(-\frac{3}{4}F + \frac{1}{2}\beta[F^2+G^2]^{1/3}G, \right. \\ \left. \frac{3}{4}G - \frac{1}{2}\beta[F^2+G^2]^{1/3}F + a\cos[\omega H], \Omega\right). \quad (14)$$

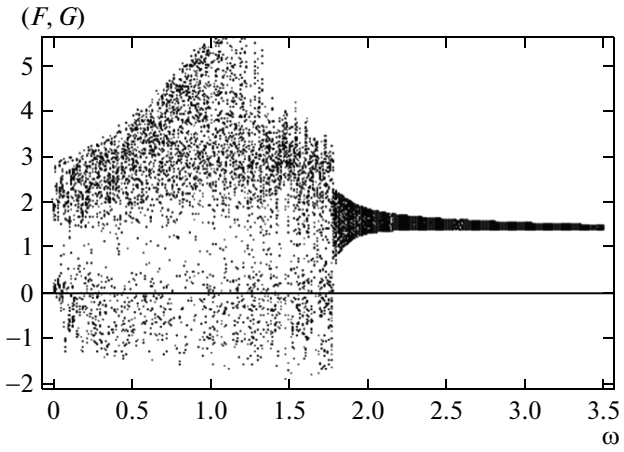

Fig. 2. Bifurcation diagram of forced GNDEs for $F(0) = 1.29904$, $G(0) = 1.29904$, $H(0) = 0$, and $a = 1$

Its divergence is seen to vanish, and therefore the flow is conserved.

It is known that bifurcation means a fundamental change in the nature of a solution and the bifurcation diagram provides a useful way to show how the behavior of a nonlinear system changes with the control parameter. For this, we build the bifurcation diagram of forced GNDEs with $F(0) = 1.29904$, $G(0) = 1.29904$, and $a = 1$ as the initial conditions (Fig. 2). At ω values smaller than 1.8, the excited Gursey instantons evidently lose their stability and show chaotic behavior. The end of chaos is visible in the vicinity of $\omega \approx 1.82$ (the critical value).

As is well known, the main traditional way for detecting chaos is the construction of a Poincaré section that provides regular and chaotic behavior regions. A regular Poincaré section consists of a few numbers of points or closed orbits that respectively denote the periodic or quasiperiodic trajectories. Numerous confused points falling on the Poincaré section mean chaos [17]. In Fig. 3, the Poincaré sections for different ω values with the initial conditions $F(0) = 1.29904$, $G(0) = 1.29904$, $a = 1$ and $\beta = 1$ are shown. The transition from chaos to regular behavior is seen at $\omega \approx 1.821$, in harmony with Fig. 2. Hence, we can conclude that external forcing having certain frequencies may change the stability characteristics of spinor-type Gursey instantons in phase space for the same initial conditions. When the forcing frequency is low enough, the Gursey instanton cannot maintain its stability for the above initial conditions.

Next, in Fig. 4, we illustrate the regular and chaotic behaviors of forced GNDEs for some random possible initial values keeping $\omega = 1.8$ and $\beta = 1$. It is interesting that the obtained phase-space display is typical for Kolmogorov–Arnold–Moser-like (KAM) dynamics, i. e., some originally periodic solutions remain regular while others start to behave chaotically [18]. In Fig. 4, we show Poincaré sections for $a = 0.2$, $a = 0.5$, $a = 1$, and $a = 1.325$. For the weak driving in Fig. 4*a*, the system shows regular behavior. As we increase the driving, Fig. 4*b* shows that the chaotic orbits appear in the region near the center of the phase space. With the driving increased further, Figs. 4*c*, *d* exhibit more chaotic regions.

It is well known that chaotic systems sensitively depend on the initial conditions, and the transitions from regular states to chaos are caused by insignificant changes in the initial conditions. To see this extreme sensitivity of forced GNDEs to initial conditions, in Fig. 5, we show the Poincaré sections corresponding to regular and chaotic behaviors for the fixed parameters $\omega = 0.8$, $a = 0.5$, and $\beta = 1$ with two different very close initial conditions. As is seen from Fig. 5*a*, the flow is a closed orbit, and hence the behavior is regular for $F(0) = 1.7$ and $G(0) = 3.67$ (in fact, quasiperiodic one). If we take another initial condition which is very close to the first one ($F(0) = 1.75$ and $G(0) = 3.7$), we observe chaotic orbits in Fig. 5*b*.

4. CLUSTER ANALYSIS OF FORCED GNDEs

As additional information, we study forced GNDEs using the hierarchical cluster analysis method. Hierarchical methods usually produce a graphical output known as a dendrogram graph, which shows the hierarchical clustering structure [19]. In Fig. 6, the dendrogram graphs belonging to hierarchical clustering of time series for solutions of forced GNDEs are shown for the fixed parameters $a = 1$ and $\beta = 1$ and the initial conditions $F(0) = 1.29904$ and $G(0) = 1.29904$ with several driving force frequencies, $\omega = 1$, 1.8, and 2. In these graphs, the x axis represents the similarity or correlation percentages (0 %–100 %) belonging to our data, $F(u)$ and $G(u)$, and increases to the right. Along the y axis, the fusion of clusters due to similarities of $F(u)$, $G(u)$ data is recorded. For each ω value, we plot the dendrogram graphs for all data values and give only the truncated dendrogram graphs that are the summary of the first 20 mergers having the same similarity percentage. For all ω values, clustering is gathered in two different main groups from the hierarchical standpoint. However, for $\omega = 1$, there are five different cluster-

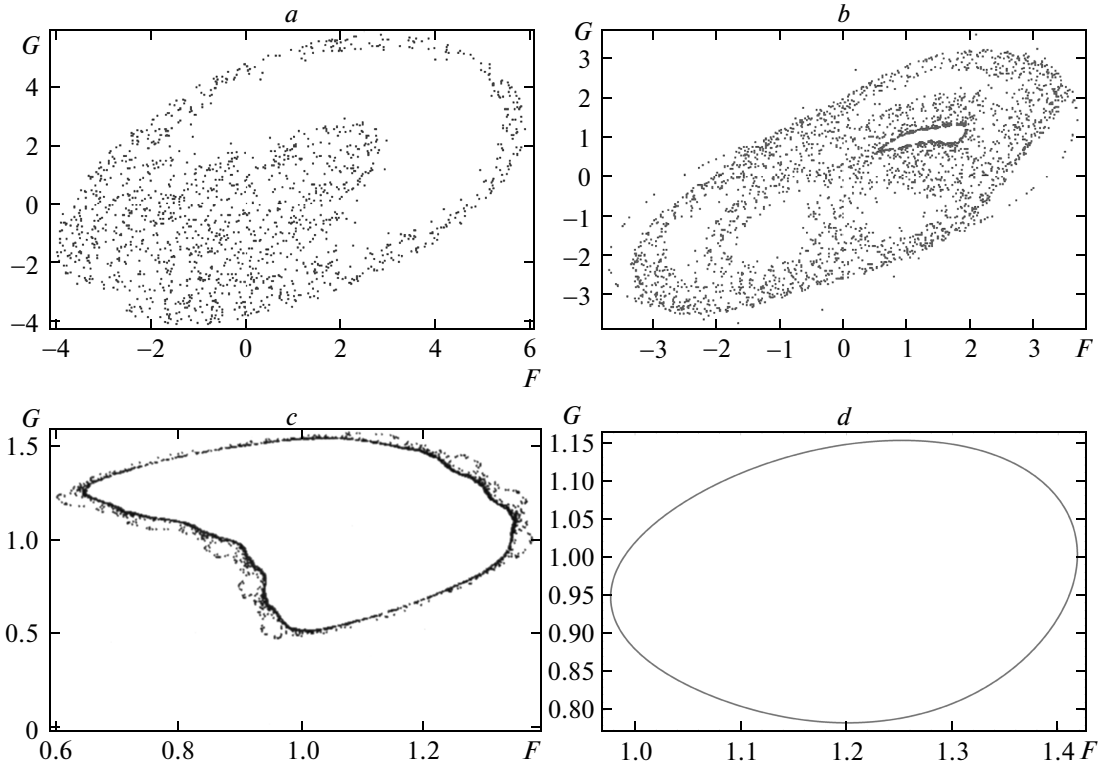

Fig. 3. Poincaré sections of forced GNDEs with the initial conditions $a = 1$, $\beta = 1$, $F(0) = 1.29904$, $G(0) = 1.29904$, and $H(0) = 0$ for various values of ω: $\omega = 1$ (a), 1.8 (b), 1.821 (c), 2 (d)

ings in the first main clustering; in the second main clustering, there are seven different clusterings. Comparably, for $\omega = 1.8$, there are five different clusterings in the first main cluster ring and eight different clusterings in the second one. On the other hand, for $\omega = 2$, there are three different clusterings in the first main cluster ring and 10 different clusterings in the second main one. Our results show that the similarity percentages between the $F(u)$, $G(u)$ data increase as the driving force frequency increases. For those ω values at which chaos occurs, i. e., $\omega = 1$ and 1.8, the data are extended in phase space and hence the cluster numbers in the truncated dendrogram graphs are higher, corresponding to the quasiperiodic behavior case.

5. CONCLUSION

More recently, the role of the coupling constant in the evolution of $4D$ spinor-type instantons in phase space has been studied via the Heisenberg ansatz [13, 14]. Moreover, a similar investigation on $2D$ Thirring instantons [15, 20] has been done [21]. Also, a comparison between $2D$ Thirring instantons and $4D$ Gursey instantons was discussed in order to understand the dependence of the behavior of spinor-type instantons in phase space on the quantum fractional spinor number and the dimension [13, 14]. To obtain more information on spinor-type instantons, we here define forced GNDEs and study their dynamical nature.

In the light of the conclusions obtained in the above-mentioned papers, the soundness of the excited instantons under external forcing acquires importance. In this paper, this is what we study, i. e., the existence of regular and chaotic numerical solutions of forced GNDEs by constructing their Poincaré sections. The obtained results show the vanishing of the stability characteristics of spinor-type Gursey instantons in phase space depending on the external forcing parameter values. The regular and chaotic behavior of forced GNDEs for various deriving force frequency values are in harmony with the bifurcation diagram. Besides, forced GNDEs exhibit more chaotic behavior depending on the increment of the forcing amplitude. The phase space of the flow possesses a KAM-like structure [18] since it is conservative. It is well known that the phase spaces having a KAM-like structure are

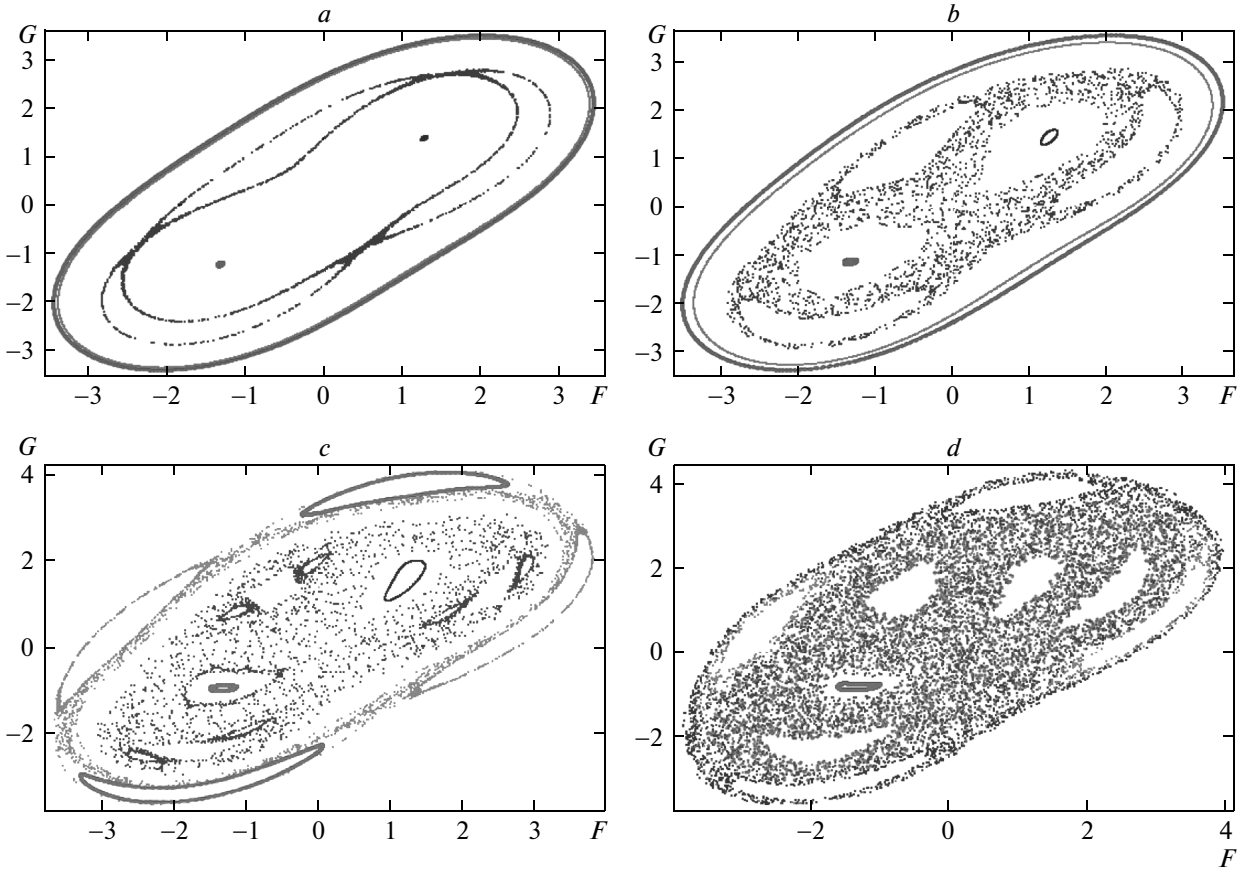

Fig. 4. Poincaré section of forced GNDEs at $\omega = 1.8$ and $\beta = 1$ for different initial conditions: $a = 0.2$ (a), 0.5 (b), 1 (c), 1.325 (d)

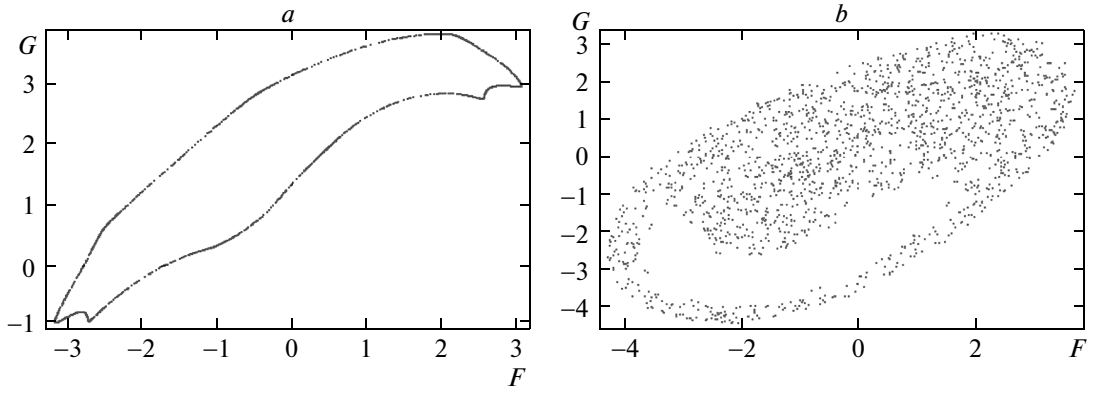

Fig. 5. Poincaré section of forced GNDEs at $\omega = 0.8$, $a = 0.5$, and $\beta = 1$: a) $F(0) = 1.7$, $G(0) = 3.67$, and $H(0) = 0$; b) $F(0) = 1.75$, $G(0) = 3.7$, and $H(0) = 0$

fundamentally different from the controlling dissipative chaotic attractors. Some originally periodic solutions remain regular and mean quasiperiodicity, while others behave chaotically. We also show that forced GNDEs sensitively depend on the initial conditions, and transitions from regular states to chaos are caused by

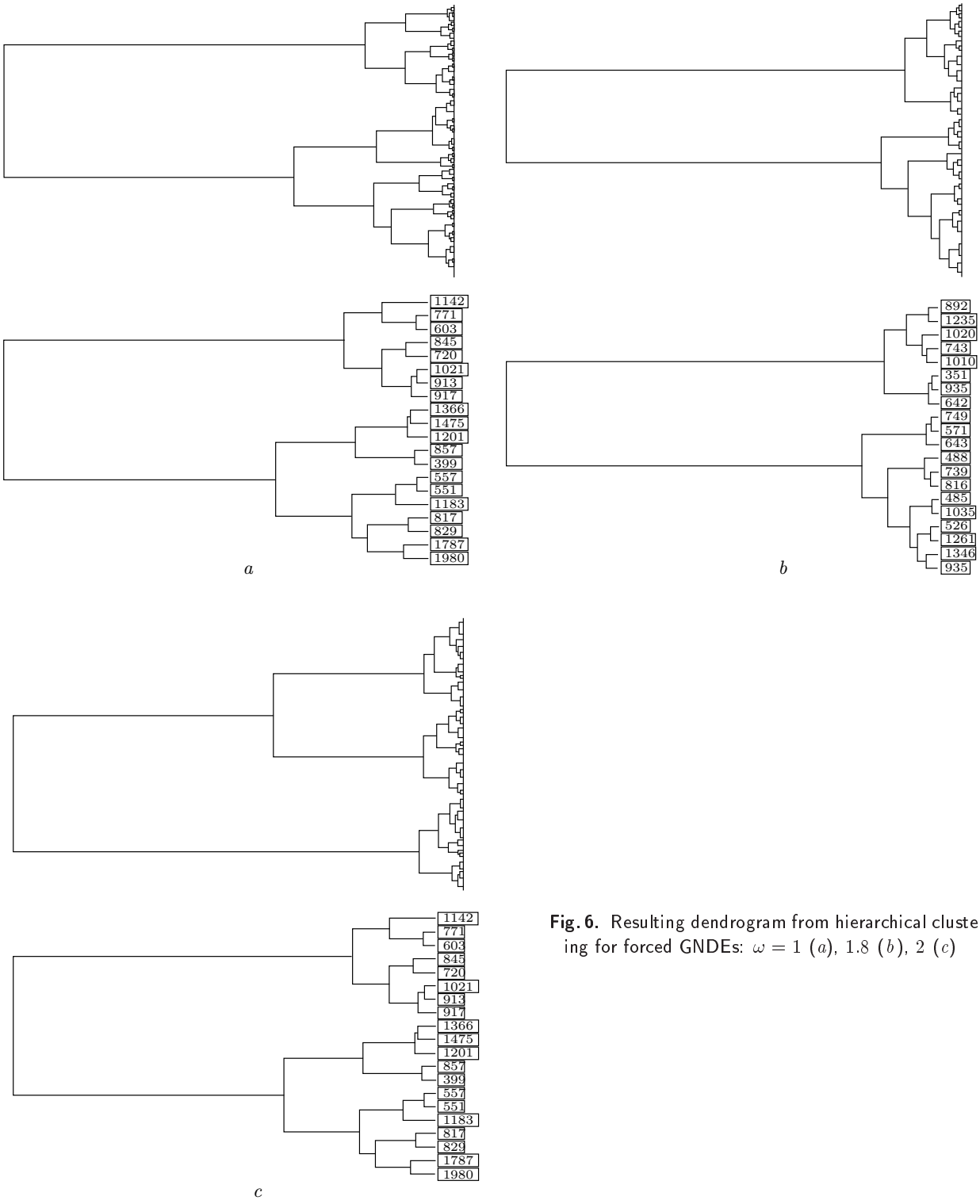

Fig. 6. Resulting dendrogram from hierarchical clustering for forced GNDEs: $\omega = 1$ (a), 1.8 (b), 2 (c)

insignificant changes in the initial conditions. Finally, the similarity percentages between the $F(u)$, $G(u)$ data increase as the driving force frequency increases with regard to the hierarchical cluster analysis investigation of forced GNDEs. The results obtained from this study lead us to the conclusion that the dynamical nature of spinor-type Gursey instantons could not be analyzed using a different method [9] whereas the method presented here makes it possible.

We thank Eren Tosyali, K. Gediz Akdeniz, and Emine Rizaoglu for their support while preparing this manuscript. This work was supported by the Scientific Research Projects Coordination Unit of Istanbul University (Project No. 35737).

REFERENCES

1. M. Dunajski, *Solitons, Instantons, and Twistors*, Oxford Univ. Press, New York (2010).
2. A. A. Belavin, A. M. Polyakof, A. S. Schwartz, and Yu. S. Tyupkin, Phys. Lett. B **59**, 85 (1975).
3. C. Houghton, *Instantons*, in the *Encyclopedia of Nonlinear Science*, Routledge, New York (2005).
4. S. Moch, A. Ringwald, and F. Schrempp, Nucl. Phys. B **507**, 134 (1997); A. Ringwald and F. Schrempp, Phys. Lett. B **438**, 217 (1998); F. Schrempp and A. Ringwald, Phys. Lett. B **503**, 331 (2001); A. Ringwald and F. Schrempp, Comput. Phys. Comm. **132**, 267 (2000).
5. W. Heisenberg, Zeits. F. Naturf. A **9**, 292 (1954).
6. F. Gursey, Nuovo Cim. **3**, 988 (1956).
7. F. Kortel, Nuovo Cim. **4**, 210 (1956).
8. K. G. Akdeniz, Nuovo Cim. **33**, 40 (1981).
9. K. G. Akdeniz, M. Arik, M. Durgut, M. Hortacsu, S. Kaptanoglu, and N. K. Pak, Phys. Lett. B **116**, 34 (1982).
10. J. Kraskievicz and ve R. Raczka, Nuovo Cim. A **93**, 28 (1986).
11. M. Soler, Phys. Rev. D **1**, 2766 (1970).
12. S. Sagaltici, Istanbul Univ., Institute of Science, Phys. Dep., M. S. Thesis (2004).
13. F. Aydogmus, Istanbul Univ., Institute of Science, Phys. Dep. Ph. D. Thesis (2012).
14. F. Aydogmus, B. Canbaz, C. Onem, and K. G. Akdeniz, Acta Phys. Polon. B **44**, 1837 (2013).
15. K. G. Akdeniz and A. Smailagic, Nuovo Cim. A **51**, 345 (1979).
16. R. Jackew, Rev. Mod. Phys. **49**, 681 (1977); A. Chakrabarti, *Introduction to Classical Solutions of Yang–Mills Field Equations* (1968).
17. M. C. Gutzwiller, *Chaos in Classical and Quantum Mechanics*, Springer-Verlag (1986), p. 132.
18. A. N. Kolmogorov, Dokl. Akad. Nauk SSSR **98**, 527 (1954); Engl. Transl.: Volta Memorial Conf. (1977), Lecture Notes in Phys. **93**, 51, Springer (1979); V. I. Arnold, Russ. Math. Surv. **18**, 13 (1963); J. Moser, Nachr. Akad. Wiss. Gött. II, 1 (1962).
19. X. Wang, K. Smith, and R. Hyndman, J. Data Mining and Knowledge Discovery, Springer (2006), p. 335.
20. W. E. Thirring, Anal. Phys. **3**, 91 (1958).
21. B. Canbaz, C. Onem, F. Aydogmus, and K. G. Akdeniz, Chaos, Solitons, and Fractals **45**, 188 (2012).